46th AIAA Aerospace Sciences Meeting and Exhibit
7 - 10 January 2008, Reno, Nevada

AIAA 2008-11

On the Connection between Near-field and Far-field Solutions of High-Speed Jet Noise

Foluso Ladeinde[a], Xiaodan Cai[b], and Ken Alabi[c]
TTC Technologies, Inc., P.O. BOX 1527, Stony Brook, New York 11790 USA

Ramons Reba[d] ,Robert H. Schlinker[e] and John Simonich[f]
United Technologies Research Center, E. Hartford, CT 06108 USA

Recent computational aero-acoustics development for high speed jet noise has focused on advanced LES methods. Validation efforts have largely been directed at comparisons in the acoustic far-field. While these results have shown encouraging levels of agreement, they bypass direct comparison on the basis of jet source characteristics. Thus, the current study aims to compare LES on the basis of multi-point statistics of jet near-field hydrodynamic pressure. A key advantage of the study is the provision for an intermediate check on the "beginning to end" simulation methodology by way of the near field measurements. High-fidelity simulations using improved low dissipation and low dispersion high-order numerical (CFD) schemes were carried out for flows from a round nozzle, with the inclusion of the nozzle in the model. Experimental measurements for the subsonic jet near-field noise assessments were obtained from a prior study led by Bridges at NASA using an array design by Suzuki and Colonius[19] with jet flows corresponding to test cases reported by Tanna[1]. Supersonic shock free near field jet noise measurements were acquired at UTRC using a novel rotating phased array system reported here for the first time. The simulated near-field results were generated directly from the RANS/LES calculations, whereas the far-field results follow from the Ffowcs Williams-Hawkings (FW-H) projection of the near-field results. Our results have shown a consistent over-prediction of the jet spreading rate. Despite this, salient qualitative features of the near-field source characteristics are captured in the simulations. Detailed analysis and resolution of the sources of discrepancy are currently in progress.

I. Introduction

Large-eddy simulation (LES) has emerged as a promising tool for predicting jet noise from large-scale turbulent structures. A recent review by Bodony and Lele [2] presents LES from various researchers, and compares the results against far-field pressure measurements of Tanna, encompassing both hot and cold subsonic jets. Researchers whose results are contained in the comparison exercise include Lew et al., [3] Lau et al., [4] Andersson et al., [5] Zhao et al., [6] Shur et al., [7,8] Bogey and Bailly, [9-13] and Ahuja et al. [14] These calculations were either compared to Tanna's measurements or to the data from Bridges and Wernet. [15] In the foregoing contributions, as well as in most others, the emphasis is primarily on validating far-field acoustic predictions

The current study aims to expand on the validation efforts presented above by providing comparisons on the basis of multi-point pressure statistics in the jet hydrodynamic near-field. The near-field pressure, measured just outside the turbulent shear layer, contains signatures of the large-scale turbulent structures (the noise source) and thus, arguably, provides a more discriminating validation metric. Moreover, such comparisons promise to provide insights into root causes for discrepancies observed in the acoustic far field. In a recent paper, we presented RANS/LES simulations

[a] Director of Research, AIAA Life Member and Associate Fellow
[b] Senior Research Engineer, AIAA Member.
[c] Research Engineer, AIAA Member
[d] Project Leader, Components Department, AIAA Member
[e] Project Leader, Components Department, AIAA Associate Fellow
[f] Staff Engineer, Components Department, AIAA Member

for hot and cold subsonic jets. In the current paper, further validation results are presented for these cases, and preliminary results are shown for a supersonic jet. We present results for Tanna subsonic set points 7 (M_j=0.9, cold) and 46 (M_j=0.56, T_j/T_{amb}=2.7), and for an ideally expanded, unheated supersonic jet (M_j=1.5). These are referred to, respectively, as SP7, SP46, and B118. Both subsonic cases have equal acoustic Mach number of 0.9.

The model, which includes both the nozzle geometry and the plume region, was calculated using a variation of the "two-stage" RANS/LES procedure described by Shur et al. [7,8,16] However, the details of our numerical schemes are different from those in Shur et al. and are described in Ladeinde et al. [17] Our procedures involve intrinsically high-order calculations of the flow and energy fields, in which the compact schemes are used for low subsonic flows and an improved (low dissipation and dispersion) weighted essentially non-oscillatory (WENO) scheme for flow fields with shock waves or strong discontinuities, as in supersonic flows. Figures 1 and 2 show the RANS and LES grids, respectively, in the hybrid RANS/LES procedure.

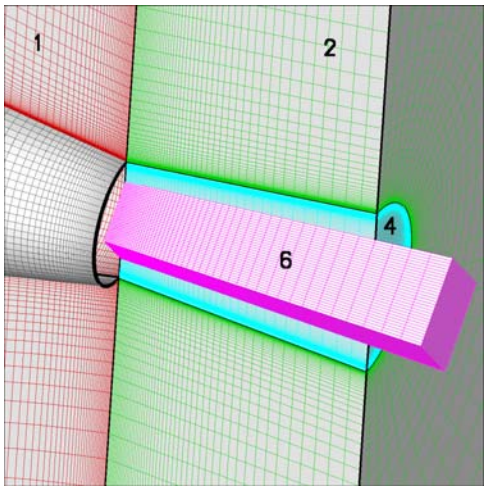

Figure 1. Computational mesh for RANS based calculation of jet flow field. Note the inclusion in the model of the inner and outer portions of the nozzle geometry. The numbers in the figure denote the computation blocks.

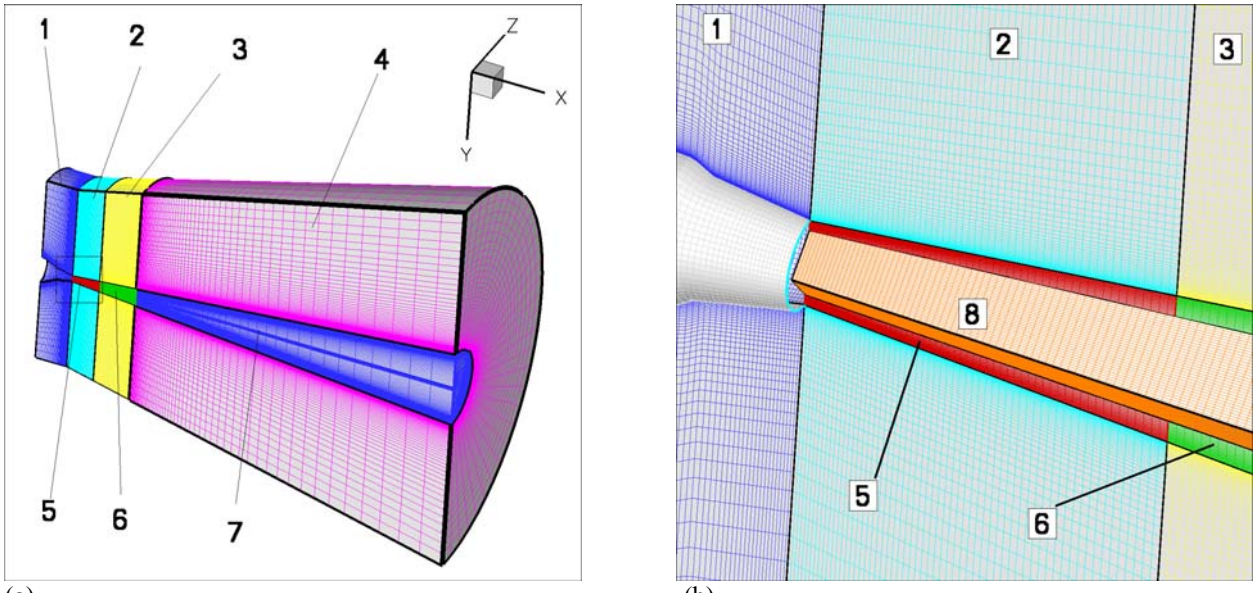

(a) (b)

Figure 2. Computational mesh for the LES based calculation of jet flow and noise. Blocks 1 through 7 are shown in (a) with half of the azimuthal planes hidden to enhance visualization. The inset in (a) is enlarged in (b)

II. Results and Evaluation

The hybrid RANS/LES procedure was first evaluated at subsonic jet exhaust velocities where recent fundamental diagnostic studies (Suzuki et al.[19]) provide extensive near-field hydrodynamic pressure data characterizing the large-scale turbulence, considered to be the source of low-frequency aft-angle sound. Predictions of near-field hydrodynamic pressure are compared to measurements reported by Suzuki[19] using a 78-microphone phased array located in the jet hydrodynamic near-field. Results for both the hot jet (Tanna SP46) and unheated jet (Tanna SP7) have been reported in Cai et al.[18] Preliminary results will also be presented for a supersonic, ideally expanded, unheated supersonic jet (M_j=1.5). For the on-going supersonic jet studies, a novel near field measurement technique was developed by UTRC to provide the analogous hydrodynamic pressure fields reported by Suzuki.

A. Flow field predictions

Subsonic conditions. Time-averaged flow quantities are shown in Figures 3 through 5. Figure 3 shows the centerline mean velocity and stream-wise turbulent intensity profiles, which are compared with the experimental data[32] and the LES results from Bodony and Lele[2] for both Set Point 7 (SP7) and Set Point 46 (SP46). Our LES results compare well with those of Bodony and Lele, which also predict a shorter potential core relative to the experimental data. Bodony and Lele attribute this discrepancy to the numerically-generated large-scale organized structures in their simulations. They argued that the organized motion of the jet column instabilities is more efficient in extracting energy from the jet than the smaller scale shear layer turbulence. They also pointed out that the numerically-imposed oscillations at the inflow boundary are different from the conditions of the experiments. In our case, numerical perturbations are not imposed at the inflow boundary. The resulting turbulence intensity level at the nozzle exit is lower than in the experiments (Figures 3, 5), although levels increase to comparable levels further downstream. We suspect that the weaker turbulence at the nozzle exit in our model could generate artificially-organized flow structures that cause a faster decay of the axial velocity.

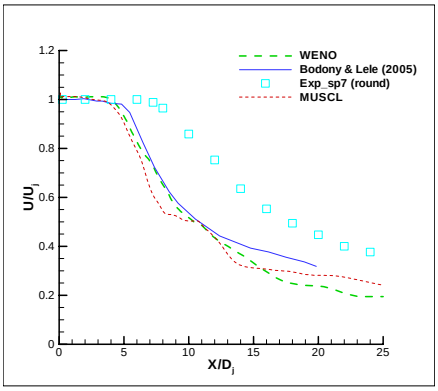

(a) Centerline velocity in cold jet

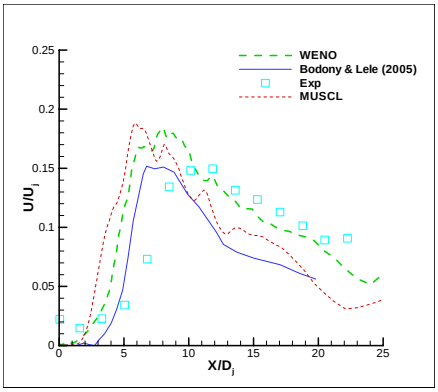

(b) Centerline stream-wise turbulence in cold jet

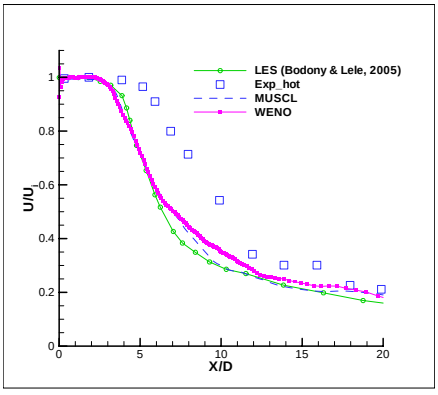

(c) Centerline velocity in hot jet

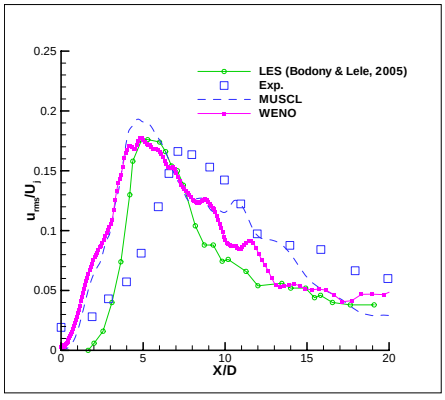

(d) Centerline stream-wise turbulence in hot jet

Figure 3. Mean centerline axial velocity and stream-wise turbulent intensity in original coordinates.

As in Bodony & Lele[21] and Bridges & Wernet[22], we use the Witze correlation[23] to re-scale the numerical data, which are then compared with the experimental data (Figure 4). This transformation is used in the form

$$\hat{x} = \kappa(x - x_c)\cdot\left(\rho_\infty / \rho_j\right)^{1/2}, \qquad (1)$$

where $\kappa = 0.08(1 - 0.16\mathrm{M_j})(\rho_\infty/\rho_j)^{-0.22}$, and x_c is a shift factor that accounts for the difference in the potential core length.

Figure 4 shows the mean centerline velocity and stream-wise turbulent intensity profiles in re-scaled coordinates. It shows that the present LES results with WENO compare well with those from Bodony & Lele[21].

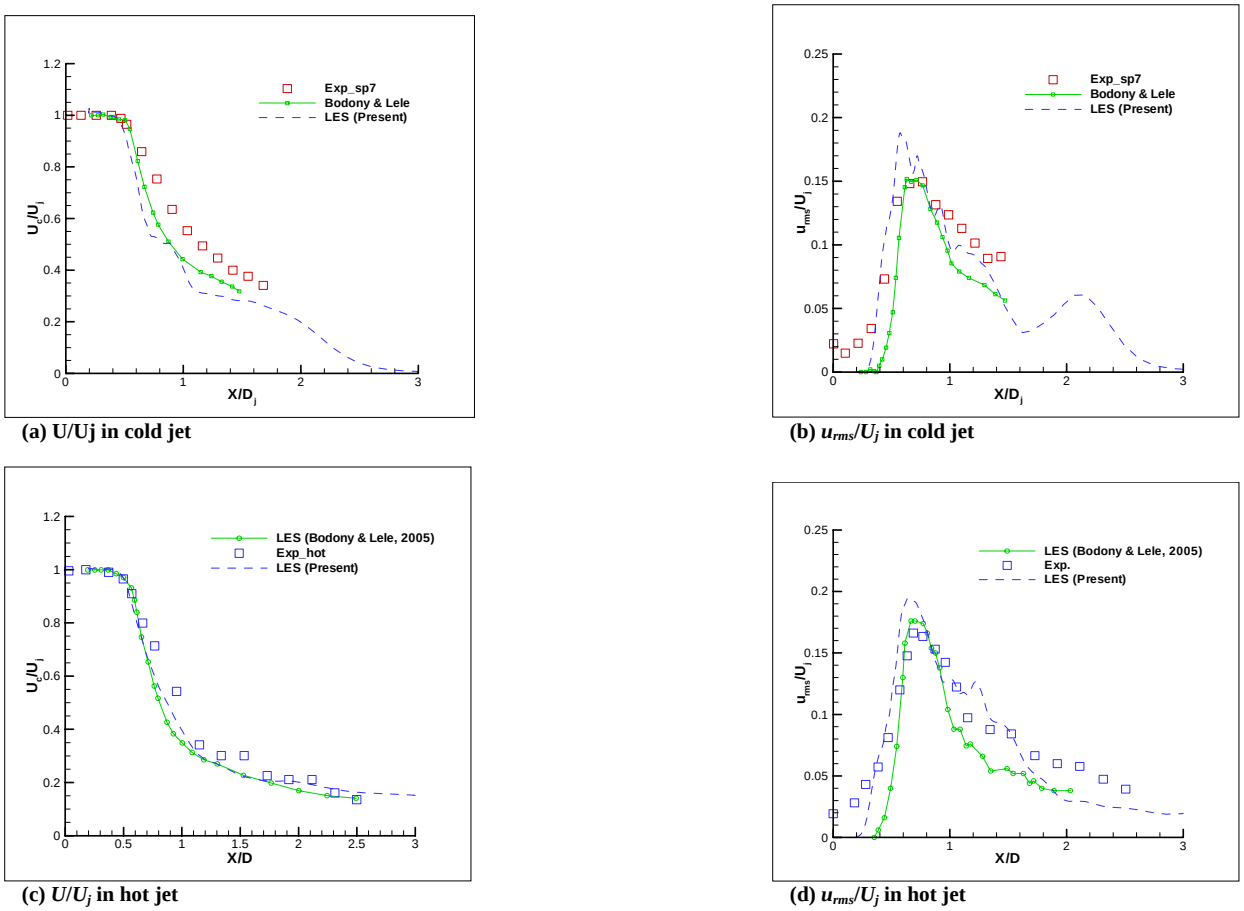

Figure 4. Centerline axial mean velocity and stream-wise turbulent intensity in rescaled coordinates.

Figure 5 compares the radial profiles of mean velocity and stream-wise turbulent intensity of the hot jet with experiments[25] at the cross-section $x/x_L = 0.5566$, where x_L is the length of the measured potential core. Agreement with the experimental data is evident.

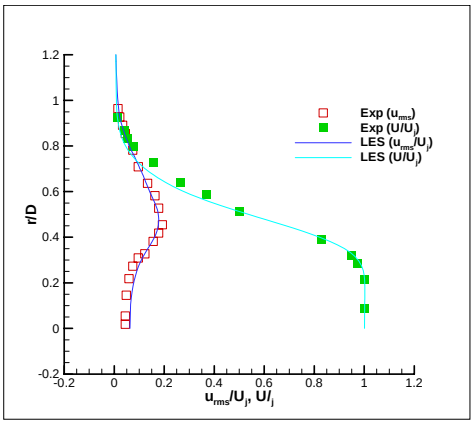

Figure 5. Radial profiles of mean velocity and stream-wise turbulent intensity of hot jet at a cross-section of x/x_L = 0.5566.

It can be concluded that the near-field velocity and turbulence results predicted by the current LES compare well with those from the LES by Bodony and Lele[21]. However, both the current LES and the simulation by Bodony and Lele under-predict the potential core lengths, which may affect the computed sound generation.

Supersonic conditions. The discrepancy in the predicted and measured mean velocity profiles has also been observed for perfectly expanded supersonic conditions. Figure 6a compares predicted centerline velocity with data acquired in the UTRC Acoustic Research Tunnel (ART) for supersonic condition B118. Radial velocity profiles were measured at *x/D*=0, 5, 10, and show faster radial spreading in the simulation, consistent with the shorter potential core length apparent in Figure 6a. Figure 6b shows that the simulation velocity profile at the nozzle exit (x/D=0) is in very good agreement with the experiment. In particular, the initial shear-layer thickness is accurately represented.

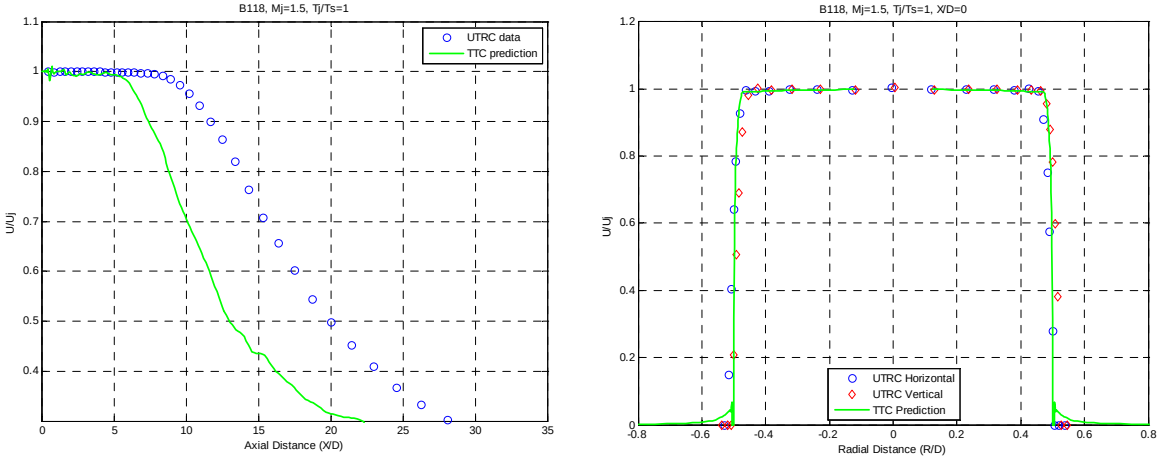

Figure 6. (a) Comparison of centerline velocity for *M*=1.5, (b) comparison of radial velocity profiles at nozzle exit *X/D*=0.0

B. Near-field Results

To assess the LES on the basis of large-scale turbulence source characteristics, we utilize the wave-packet framework of Reba et al. [18] This experimental-diagnostic method was previously used to establish quantitative cause-and-effect relationships between the characteristics of large-scale turbulence and far-field sound. For the sub-sonic validation cases, we used raw time-series data from the hydrodynamic array of Suzuki et al.[19]. For supersonic jet conditions, near-field data was acquired using a novel rotating array system (Figure 6) developed at UTRC. The technique consists of two linear arrays, one fixed, and one rotating around the jet axis. Data can be simultaneously acquired at any rotation angle to provide localized near field pressure data/spectra and multi-point correlation

measurements for extraction of large-scale turbulence wave-packets. Further details on the rotating array and its application to supersonic jets will be presented in a forthcoming paper.

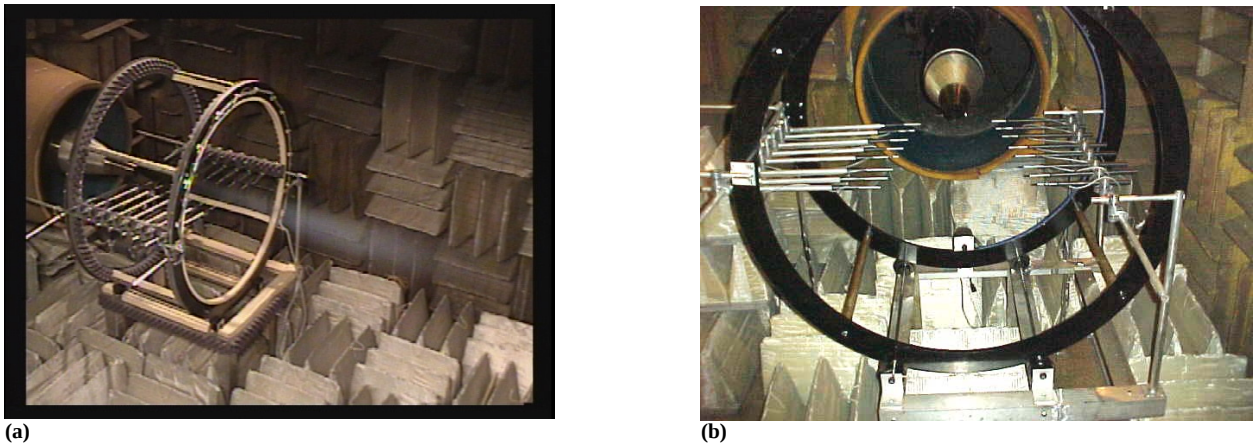

(a) **(b)**

Figure 7. (a) Rotating array configuration installed in UTRC Acoustic Research Tunnel high speed subsonic and supersonic nozzle experiments; (b) view looking upstream into 36 inch diameter open jet wind tunnel with rotating array in plane of reference microphones.

The critical step in the wave-packet approach is to construct the two-point correlation of hydrodynamic pressure on a conical surface $r_0(x)$ surrounding the jet plume

$$R_m(x_1, x_2, \omega) = \int < p_m^*(x_1, r_0, t) \cdot p_m(x_2, r_0, t+\tau) > e^{i\omega\tau} d\tau \,, \tag{2}$$

where the subscript m indicates azimuthal mode number.

Subsonic jets. Figure 8 compares wave-packets computed from LES with the experimental data for SP46 (heated subsonic jet). Due to statistical uncertainty related to the duration of time series available from the simulation, a quantitative comparison is difficult to make. However, it can be seen that distances between the wave-packet peaks and troughs are comparable in the LES and experiment, indicating that the LES captures the wavelength of the large-scale structures. It is also apparent in this result that the simulated wave-packets peak slightly upstream as compared to the experimental data, consistent with the shorter potential core in the simulation.

Comparisons of single-point pressure spectra along the array (i.e. R_m at x_1=x_2) for SP46 are shown for azimuthal mode m=0 in Figure 9. In all cases, the LES results have been plotted with a correction of –10dB. However, it is apparent that agreement between LES and experimental data is very good in terms of spectral shape. In particular, evolution of the spectral shape and relative amplitude with down-stream distance is captured. As expected, for *St* beyond ~1, the simulated spectra experience a more pronounced roll-off as compared to the experimental data, consistent with the coarse grid used in the simulation. It is apparent that the LES has a significant tonal component in the near-nozzle region absent in the experiment. This may indicate that the initial shear layer region in the simulation has a more transitional character than in the experiment.

Comparisons of single-point pressure spectra along the array (i.e. R_m at x_1=x_2) for SP7 (cold subsonic jet) are shown for azimuthal modes m=0,1,2 in Figures 10, 11, and 12, respectively. In all cases, the LES results have been plotted with a correction of –5dB. Again, the agreement in terms of spectral shape is quite good. Comparisons at m=2 show generally more pronounced discrepancies with experiment in terms of spectral shape.

R_m for SP7 derived from LES and from experimental data is compared in Figure 13 for m=0. Again, due to the statistical uncertainty in the LES (related to the relatively short time series), quantitative comparisons atre difficult to make. However, the qualitative comparison is quite good.

Corresponding results for m=1 and m=2 are shown in Figures 13 and 14. It can be seen that general qualitative features are captured. In particular, LES captures the trend of more rapid spatial de-correlation with increasing mode order.

Supersonic jet. We next present results for an unheated supersonic jet (M_j=1.5, cold). Comparisons of near-field pressure spectra along the rotating array (i.e. R_m for x_1=x_2) between experimental data and LES predictions are shown in Figure 16. In contrast with the above subsonic comparisons, significant discrepancies are apparent in terms of spectral shape. Significant discrepancies also occur at lower frequencies, while fairly good (quantitative) agreement is seen at higher frequencies for some of the axial locations. As mentioned earlier, the LES has a significantly shorter potential core, consistent with the higher levels of unsteadiness in the near-field data.

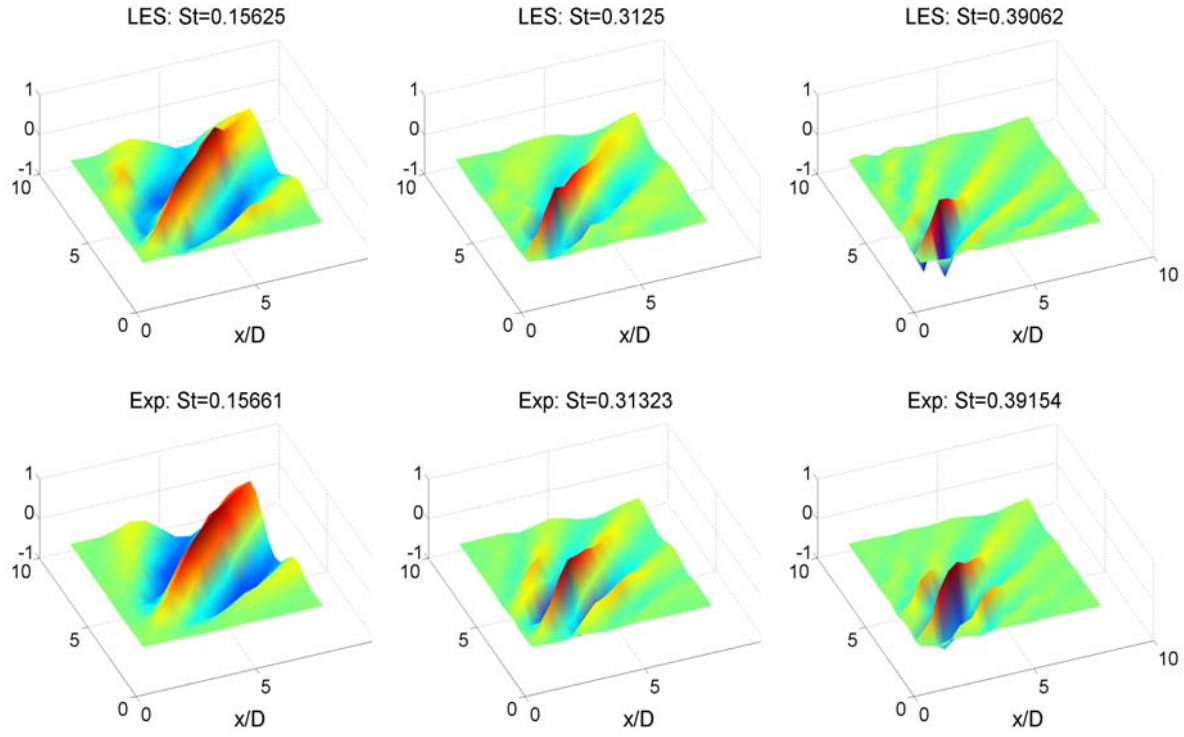

Figure 8. Real part of *Rm* for Tanna Sp 46. LES (top) compared to experiment (bottom); *m*=0.

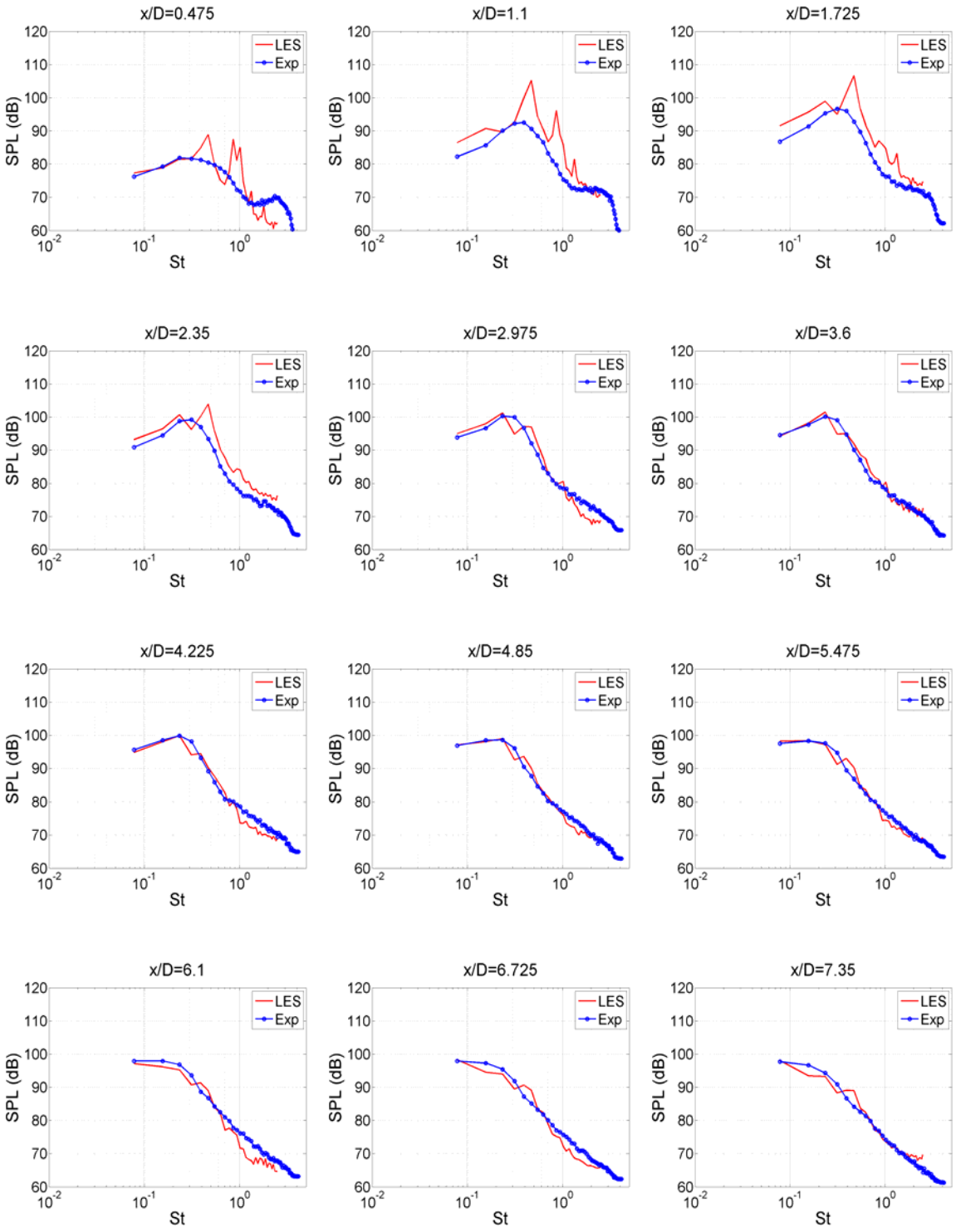

Figure 9. Comparison of measured and simulated pressure spectra along hydrodynamic array for Tanna SP46; *m*=0; LES results have been shifted by –10dB.

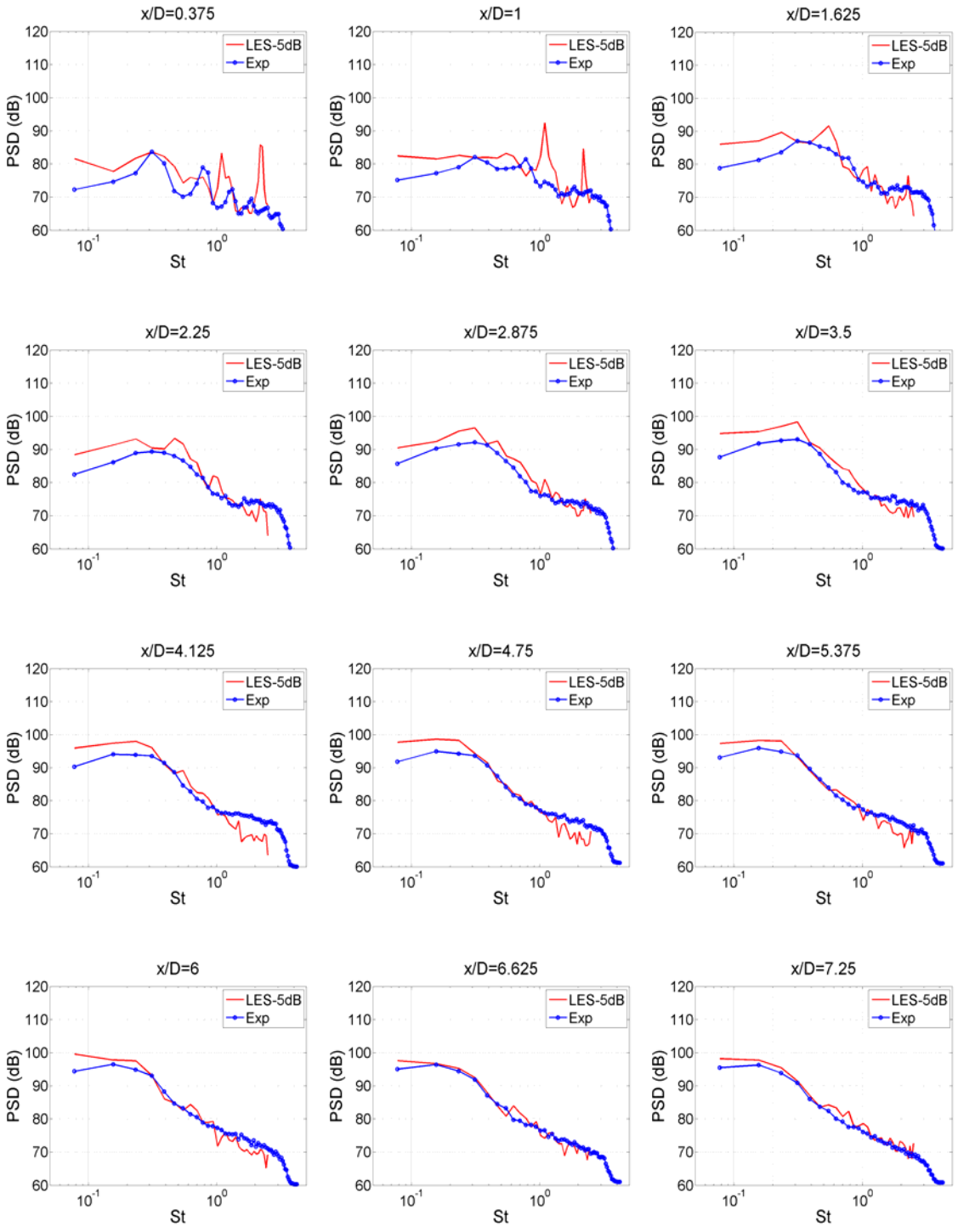

Figure 10. Comparison of measured and simulated pressure spectra along hydrodynamic array for Tanna SP7; *m*=0; LES results have been shifted by –5dB.

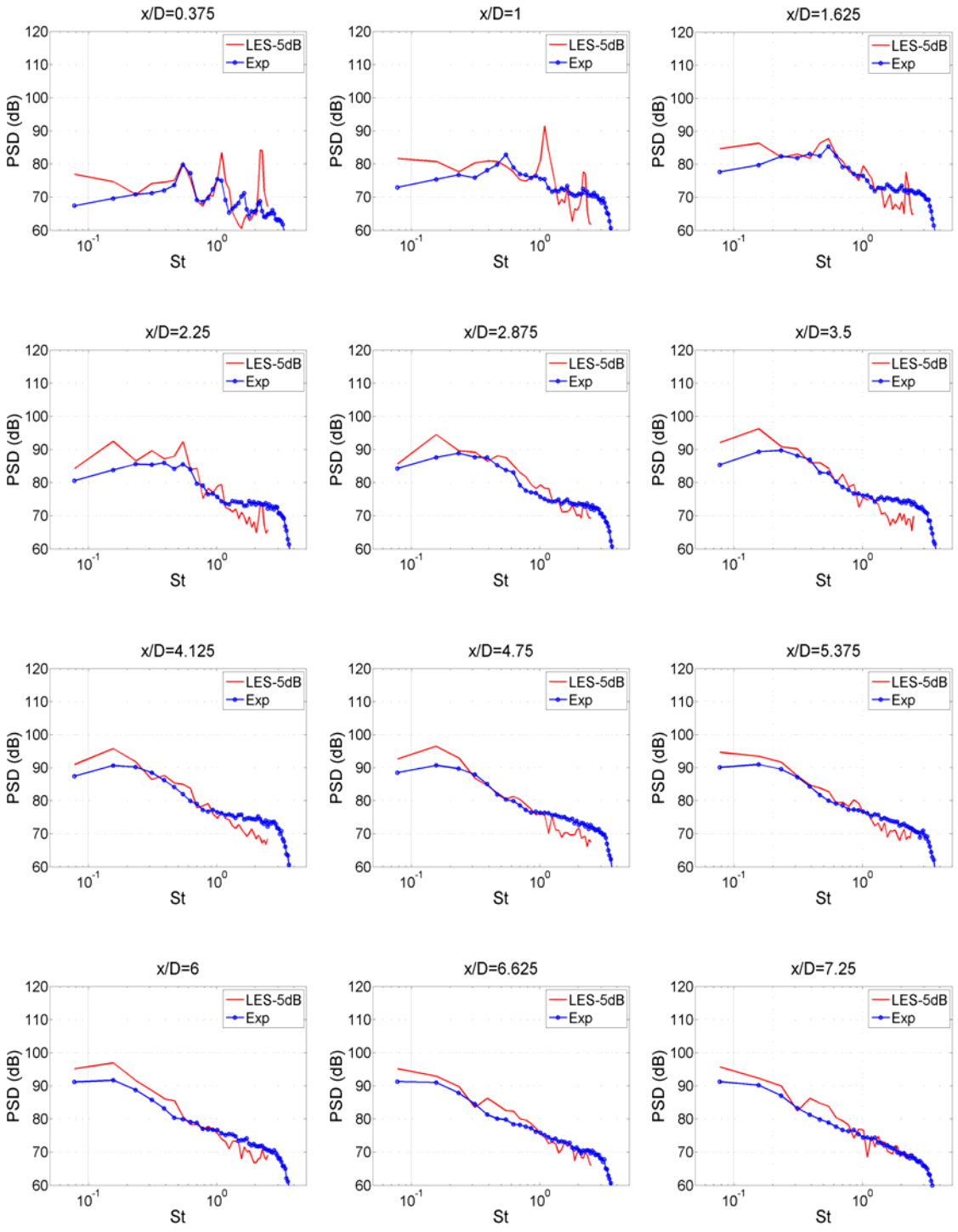

Figure 11. Comparison of measured and simulated pressure spectra along hydrodynamic array for Tanna Sp 7; *m*=1; LES results have been shifted by –5dB.

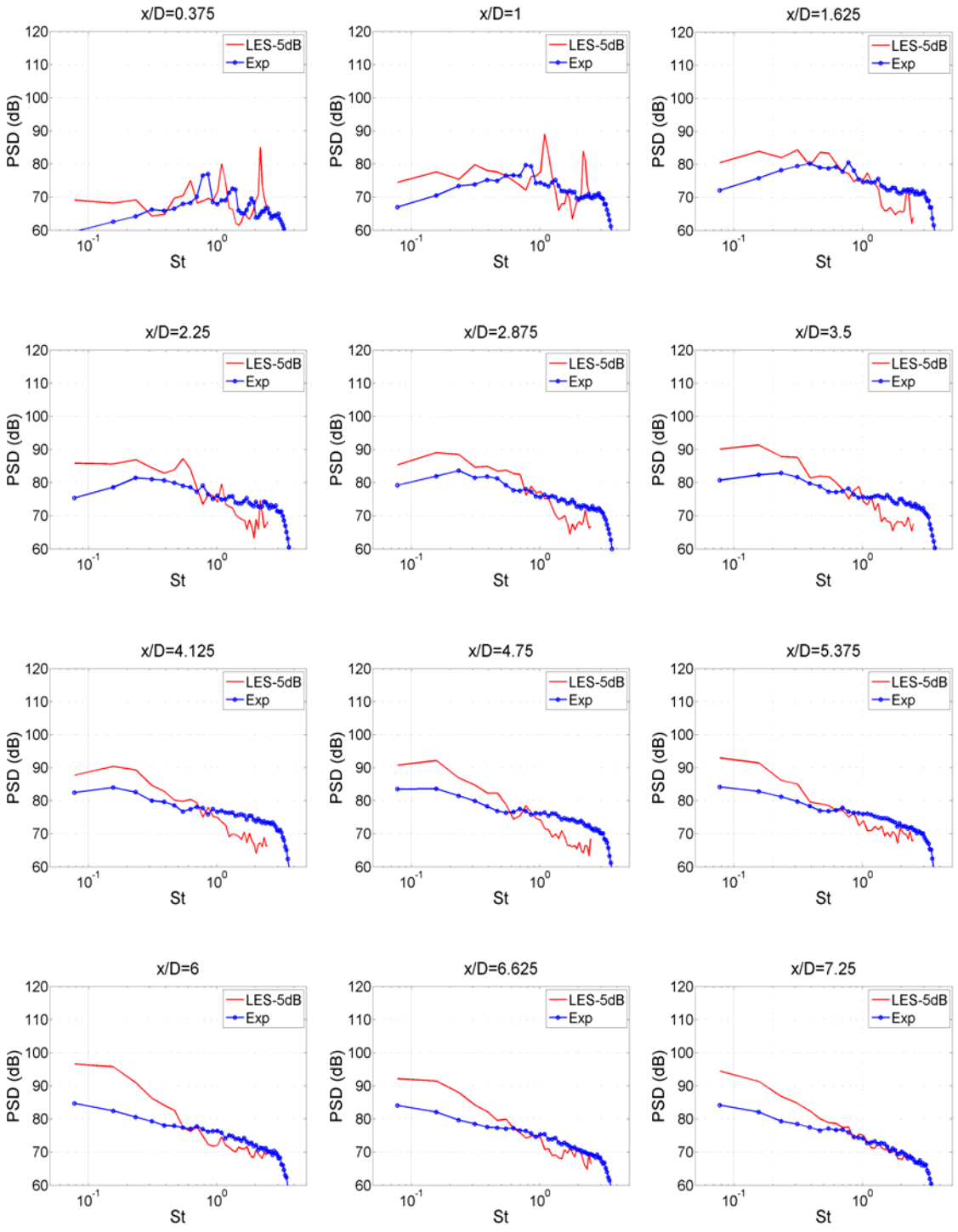

Figure 12. Comparison of measured and simulated pressure spectra along hydrodynamic array for Tanna Sp 7; *m*=2; LES results have been shifted by –5dB.

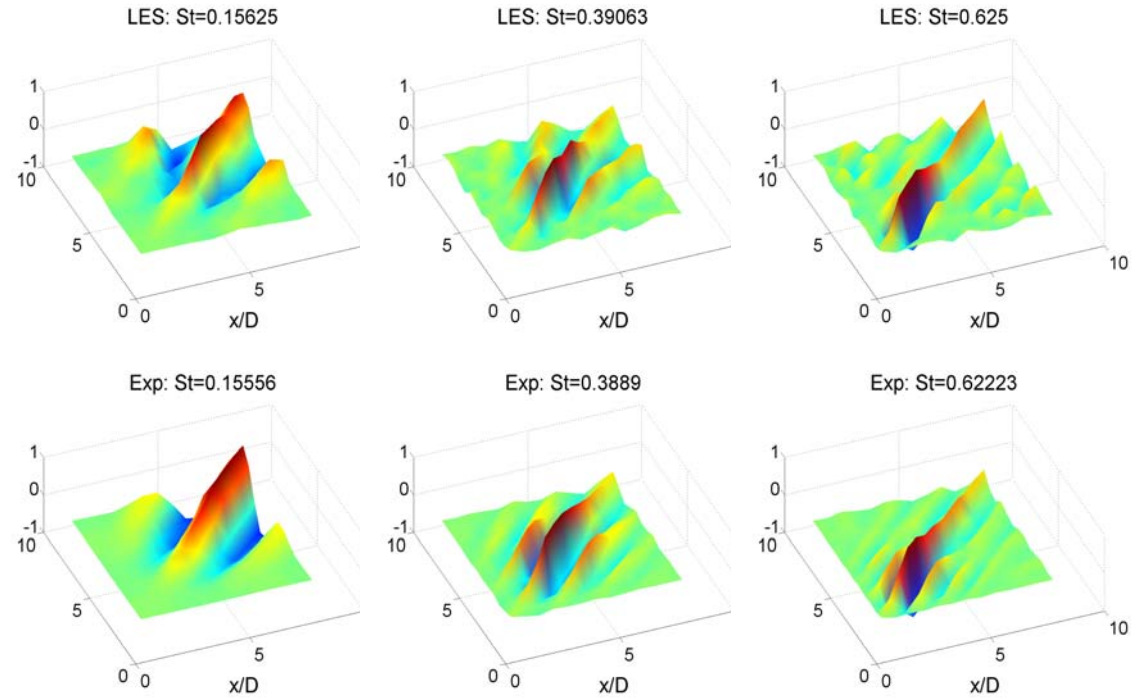

Figure 13. Real part of *Rm* for Tanna Sp 7. LES (top) compared to experiment (bottom); *m*=0.

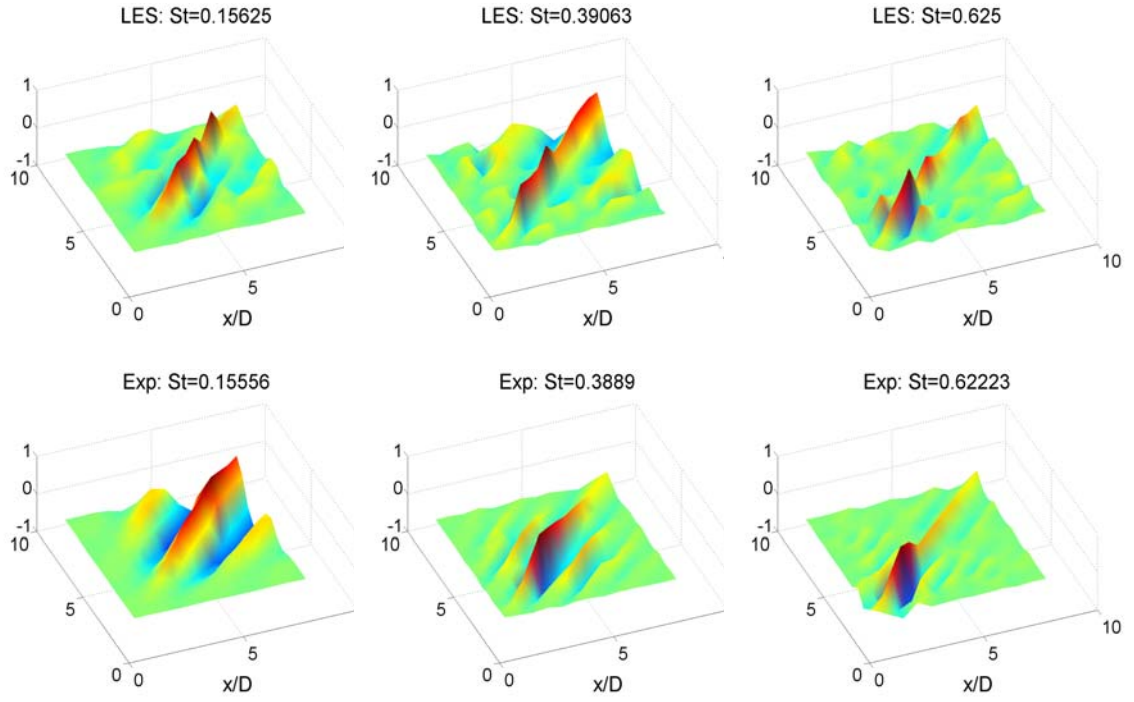

Figure 14. Real part of *Rm* for Tanna SP7. LES (top) compared to experiment (bottom); *m*=1.

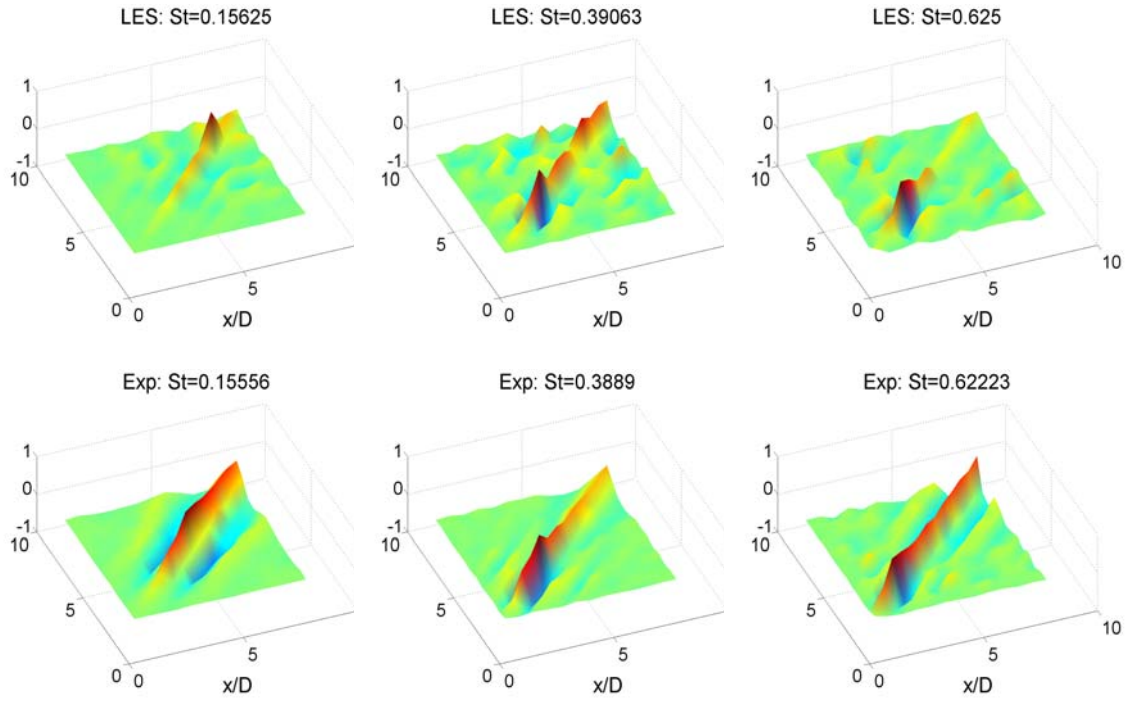

Figure 15. Real part of *Rm* for Tanna SP 7. LES (top) compared to experiment (bottom); *m*=2.

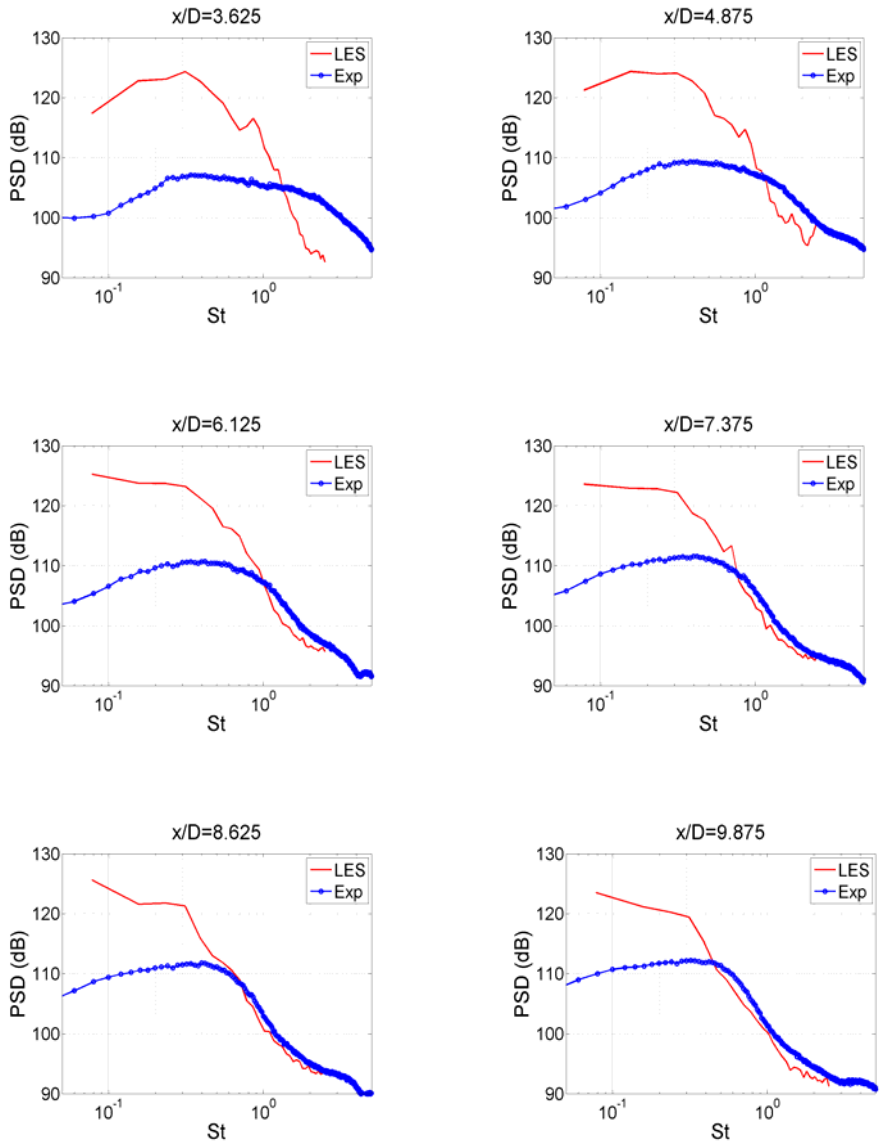

Figure 16. Comparison of measured and simulated supersonic pressure spectra along near-field array (B118). All azimuthal modes.

C. Far-field Analysis

The far-field acoustics are obtained by the Ffowcs Williams-Hawkings projection method, which can be written as

$$4\pi|1-M_r\|\vec{x}|\cdot p'(\vec{x},t)= \quad p'_Q(\vec{x},t)+\frac{x_j}{|\vec{x}|c_0}\frac{\partial}{\partial t}\int_S\left[p'n_j+\rho u_j(u_n-V_n)\right]_{ret}dS+ \\ \frac{\partial}{\partial t}\int_S\left[\rho_0 u_n+\rho'(u_n-V_n)\right]_{ret}dS, \tag{3}$$

where p'_Q is the quadrupole noise due to turbulent stresses, which could be neglected in the potential flow region. The subscript "*ret*" refers to the quantities in the brackets taken at the retarded time. In Eqn. (3), the subscripts *r* and *n* indicate the component of vectors in the radial direction ($\vec{r}$) and the surface normal directions ($\vec{n}$), respectively. The flow velocity is u_i, V_i is the velocity of the control surface, and $M_r = \vec{V} \cdot \vec{x} / \left(c|\vec{x}|\right)$.

To assess the numerical errors introduced by the far-field approximations in Eqn. (3), and to validate the numerical procedure, a monopole sound propagating wave is first tested. The monopole sound wave satisfies the equation

$$\frac{\partial^2 \Phi}{\partial t^2} = c^2 \nabla^2 \Phi \ , \tag{4}$$

where Φ is the potential function. The pressure of the sound wave has the form

$$p = -\rho_0 \frac{\partial \Phi}{\partial t} = \frac{1}{R} \sin\left(\omega\left(t - \frac{R}{c_0}\right)\right),$$

where all variables are non-dimensional and *R* is the distance from the monopole sound source as shown in Figure 17. The Ffowcs Williams-Hawkings integration surface is located at *R*=1.5. Figure 18 shows the predicted sound pressures at P1 (R=20) and P2 (R=50), compared with the analytical solution. Excellent agreement can be observed, showing that the present FW-H approach is potentially very accurate.

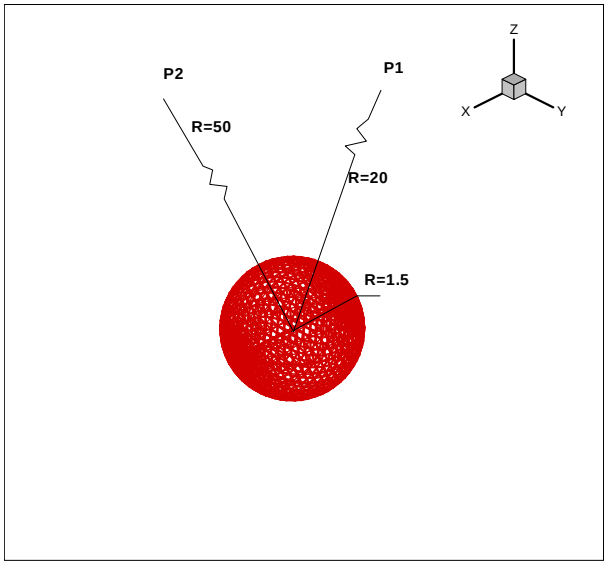

Figure 17. Sketch of FW-H integration of monopole sound wave.

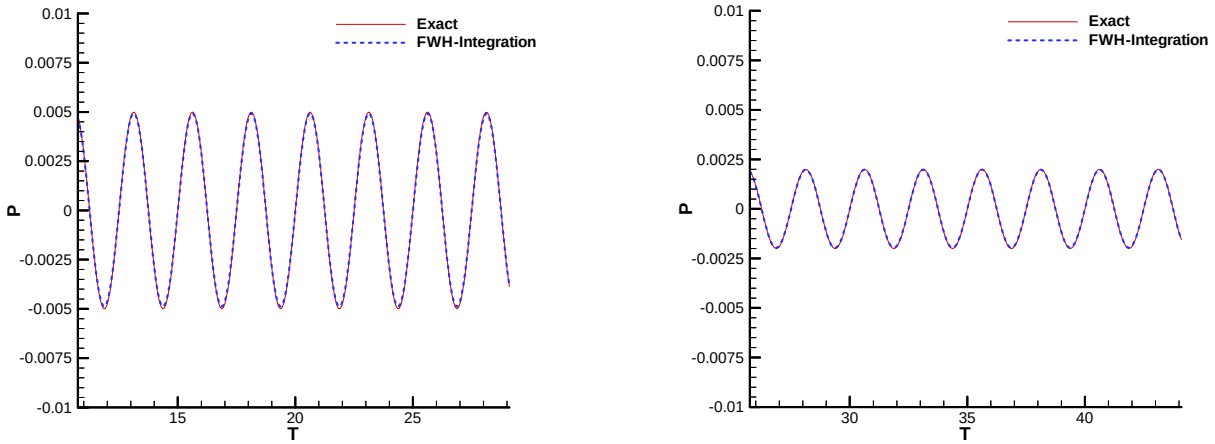

(a) (b)

Figure 18. Far-field sound pressure obtained with the FW-H integration methods: (a) R=20; (b) R=50.

As is known theoretically, the exact location of the FW-H integration surface should not play a role in predicting far-field sound if all of the terms in the equation are accounted for. However, in our numerical implementation, Eqn. (3) is only approximately accurate as the quadrupole term is neglected and all the terms of $O(1/r^2)$ are ignored. Therefore, it is essential to check the effects of the FW-H integration surface locations on the results of integration. Figure 19 shows the locations of the FW-H integration surfaces in our subsonic and supersonic jet simulations. The effects of FW-H integration surfaces on OASPL values are demonstrated in Figure 20 for SP7. It shows that the downstream location of the FW-H integration surface affects the small-angle OASPL values, and the radial location affects the large-angle OASPL. The effects of the location of the integration surfaces are larger for the WENO scheme than for the MUSCL scheme. It can be noted that the high frequency part of the SPL spectra is more dissipated when the FW-H integration surface is located farther away from the active jet flow regions, where the grid size has also been coarsened.

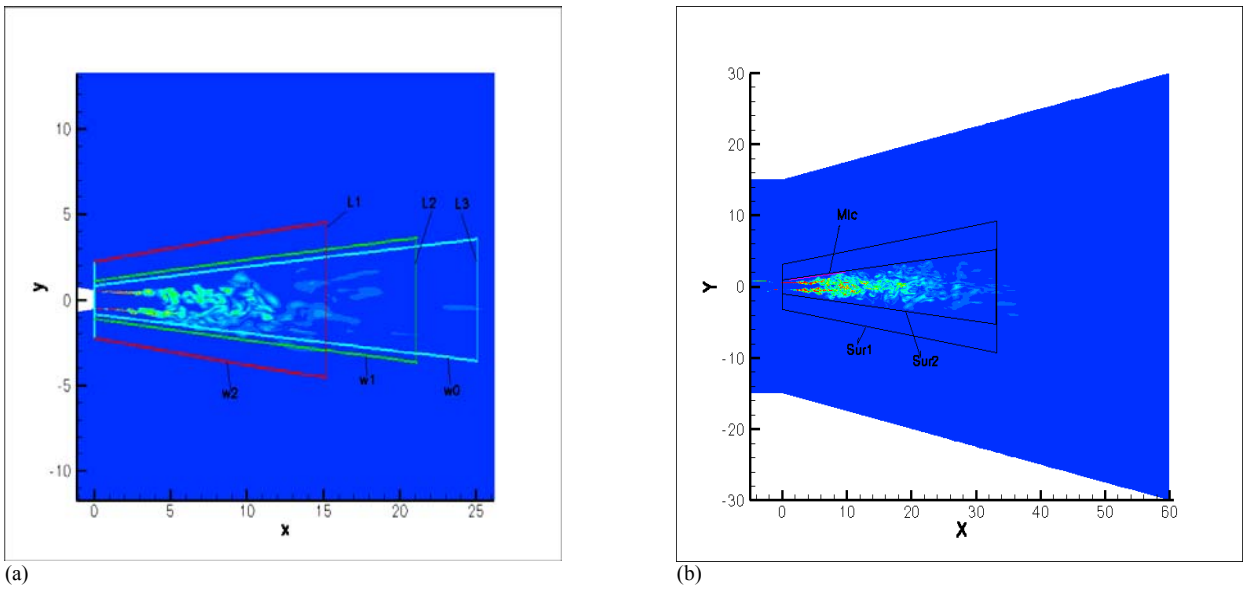

(a) (b)

Figure 19. Various Ffowcs Williams-Hawkings surfaces. (a) subsonic jets; (b) supersonic jets.

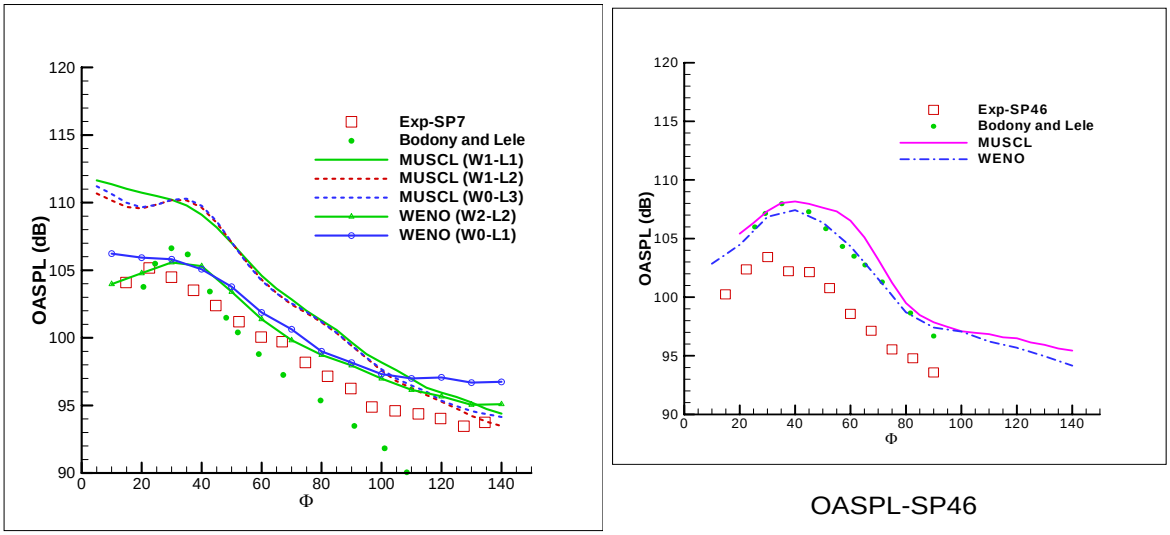

Figure 20. OASPL for SP7 (left) and SP46 (right) from different FW-H surfaces. SP46 result has over-prediction of roughly 5dB.

Figure 21 compares the predicted far-field power spectral density (using the above FW-H method) against measurements for SP7. We note that, unlike the corresponding near-field data shown in Figures 10, 11 and 12, no shifting of the LES results was applied in Figure 21. Agreement between the measurement and simulation is quite good at the aft-most angles. At the more side-ward angles, there is a pronounced over-prediction, producing an apparent "broadening" of the directivity pattern. Prior analysis using the wave-packet framework (Reba et al. [18]) has shown that a similar directivity broadening, known to occur with jet heating, can be attributed to shortening of the wave-packet streamwise correlation scale. This observation suggests that the directivity broadening seen here may fundamentally be the result of the contraction of the wave-packet, related in turn to the artificial shortening of the potential core by the increased mixing rate. In essence, the increased mixing mimics some of the acoustic effects of heating.

Analogous comparisons of far-field power spectral density are shown in Figure 22 for the supersonic condition B118. Again, comparisons at the aft-most angles appear reasonably good. However, significant over-prediction is apparent at other angles, consistent with the over-prediction of near-field pressure. As in the SP7 case, there is an apparent "broadening" of the directivity pattern.

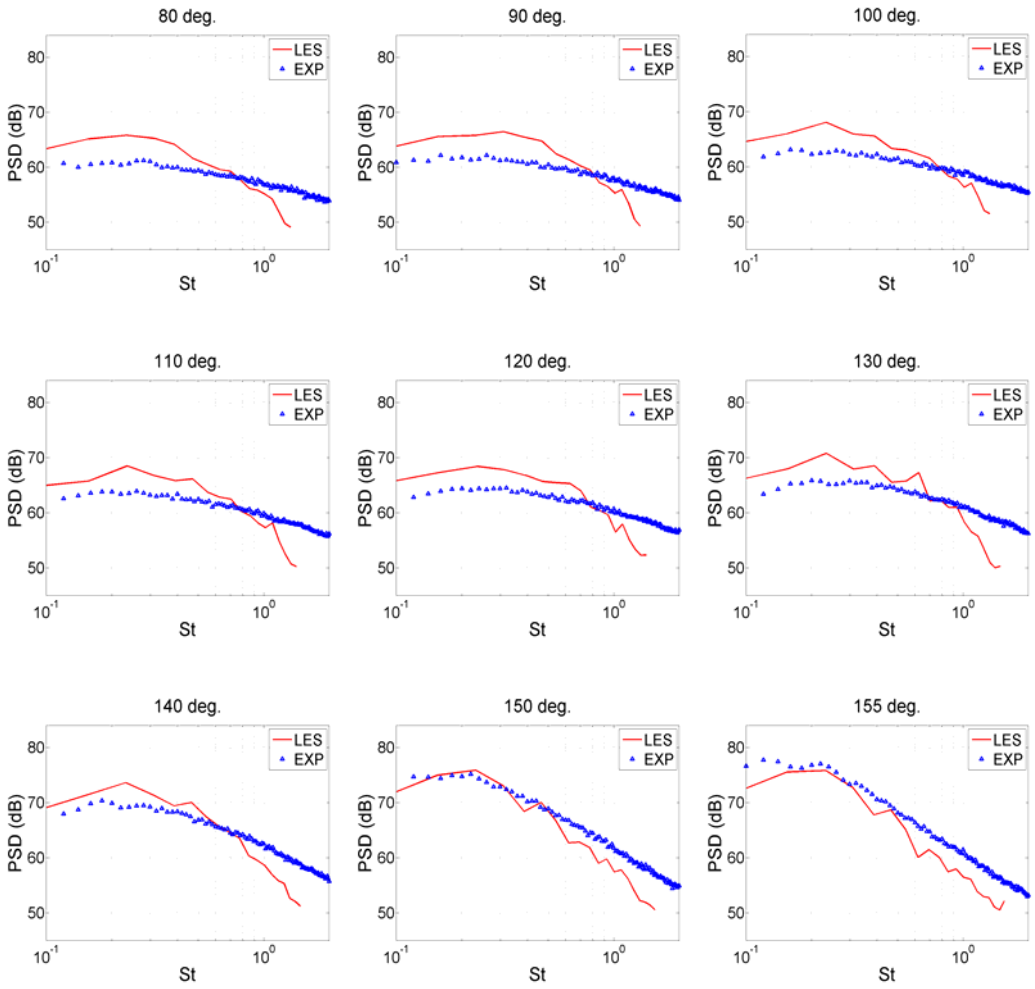

Figure 21. Comparison of measured and simulated subsonic pressure spectra along far-field array for SP7 (angles relative to inlet axis)

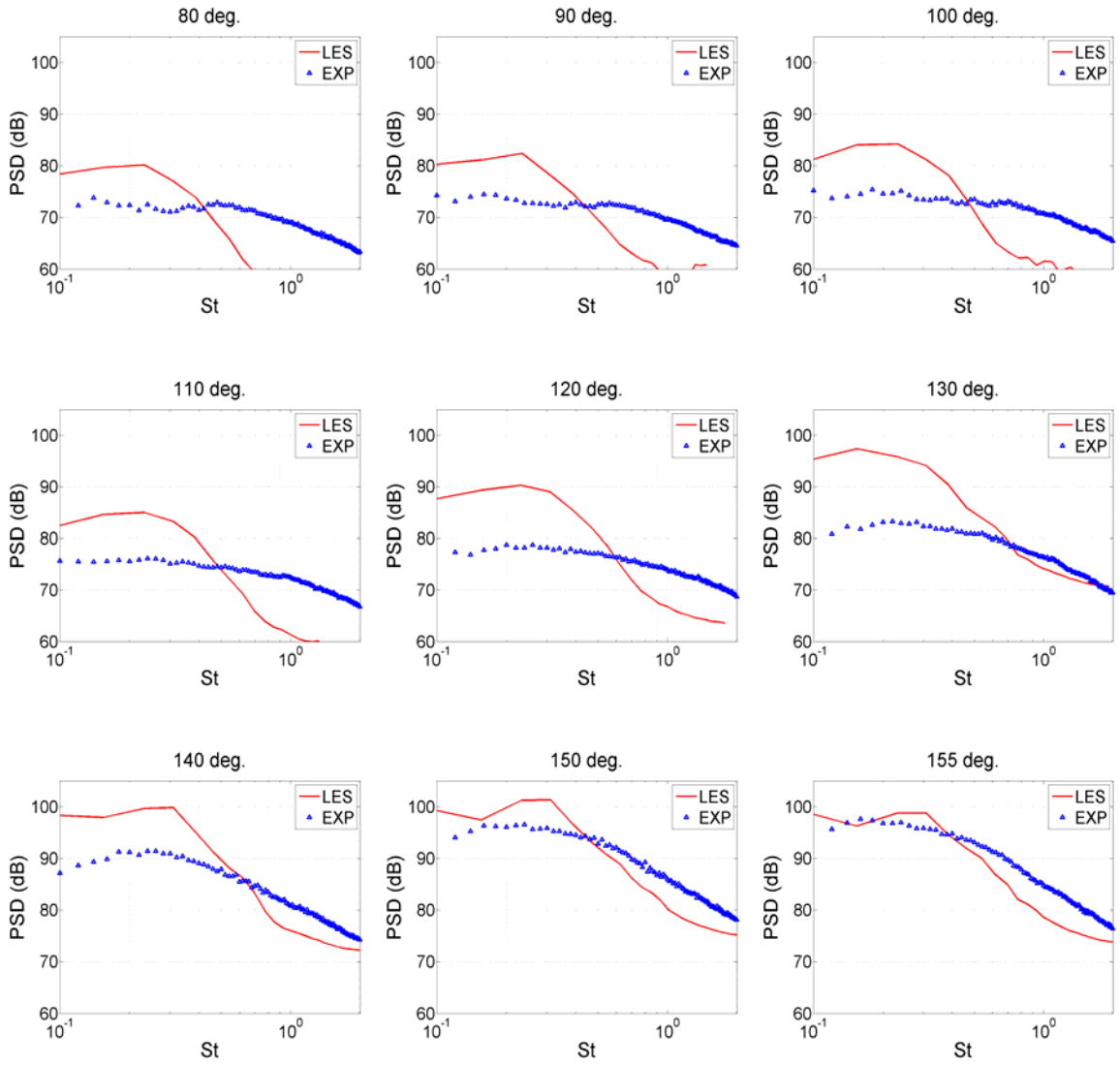

Figure 22. Comparison of measured and predicted far-field pressure for set point B118 (angles relative to inlet axis)

III. Discussion

Several observations can be drawn from the current study. First, existing validations of LES predictions for high speed jet noise are primarily based on a comparison of the far-field spectra, without a corresponding focus on the near field. The results in this paper show that, in some cases, the far-field predictions agree better with the experiments than do the near-field. Thus, comparisons on the basis of near-field source characteristics offer a more discriminating metric. Another comment pertains to the low emphasis that is given to the errors from simulations, even for the far-field results. This is unfortunate because some of the errors that we have observed in many calculations reported by others are actually of larger magnitudes that the target noise reduction levels, suggesting a need to improve the accuracy of those calculations.

The results in this paper indicate that our simulation captures the spatio-temporal evolution of large-scale turbulence with reasonable accuracy. However, the LES-predicted turbulence structures appear to be significantly more energetic. It was consistently found that the predicted potential core lengths are about two jet diameters shorter than the experimental data, and the turbulence intensities distributed at the jet axis-centerline are higher than the experimental data. These observations are consistent with those from earlier LES by others (Bogey and Bailly[20], Bodony and Lele[21]). As a result, an over-prediction of 5 and 10dB is observed in the near-field pressure for the cold and hot jet simulations, respectively. For the far-field sound pressure, the LES-predicted OASPL agrees with the

experimental data very well for the cold jet, and over predicted the hot-jet sound level by 5dB. It is noted that similar discrepancies have been reported by others applying LES to subsonic heated jets [3-4]. The near-field results for the supersonic calculations show significantly high noise levels, particularly at low frequencies. In the far field, reasonable agreement is seen at the aft-most angles, while over-predictions are seen at the more sideward angles.

A consistent trend in all simulations completed by our group to-date is the shortening of the potential core length due to an artificially high mixing rate. Despite this, salient qualitative features of the near-field source characteristics are captured in the simulations**.** Detailed analysis and resolution of the sources of discrepancy are currently in progress, with emphasis on the role of inflow conditions to the LES domain.

IV. Acknowledgements

This work is supported by the US NAVY SBIR contract N68335-07-C-0017, with Dr. John Spyropoulos as Technical Monitor. We would like to acknowledge Drs. James Bridges and Sang Soo Lee for performing the experiments at Glenn. The first author would like to express his appreciation to the following colleagues for the useful discussions he had with them on near-field simulation error: Profs. S. Lele and D. Bodony and Drs. A. Uzun, and P. Spalart. The contribution of Prof. T. Colonius is also acknowledged.

References

[1]Tanna, H.K. "An Experimental Study of Jet Noise Part I: Turbulent Mixing Noise," *J. Sound Vib.*, Vol. 50, No. 3, 1977, pp. 405-428.

[2]Bodony, D. and Lele, S. "Review of the current status of jet noise predictions using large-eddy simulation," AIAA 44th Aerospace Sciences Meeting and Exhibit, 9-12 January, 2006, Reno, NV.

[3]Lew, P., Blaidell, G. A., and Lyrintzis, A. S. "Recent progress on hot jet aeroacoustics using 3D large-eddy simulation," AIAA Paper 2005-3084, Presented at the 11th AIAA/CEAS Aeroacoustics Conference and Exhibit, May 23-25, 2003.

[4]Lau, J.C., Morris, P.I., and Fisher, M.J., "Measurements in subsonic and supersonic free jets using a laser velocimeter," *J. Fluid Mech.*, Vol. 93, No. 1, 1979, pp. 1-27.

[5]Andersson, N., Eriksson, L.-E., and Davidson, L., "A Study of Mach 0.75 Jets and Their Radiated Sound Using Large-Eddy Simulation," AIAA Paper 2004-3024, Presented at the 10th AIAA/CEAS Aeroacoustics Conference and Exhibit, Manchester, U.K., 10-12 May, 2004.

[6]Zhao, W., Frankel, S.H., and Mongeau, L., "Large Eddy Simulations of Sound Radiation from Subsonic Turbulent Jets," *AIAA J.*, Vol. 39, No. 8, 2001, pp. 1469-1477.

[7]Shur, M., Spalart, P.R., and Strelets, M.K., "Noise Prediction for Increasingly Complex Jets. Part I: Methods and tests," *Inter. J. Aeroacoustics*, Vol. 4, No. 3-4, 2005, pp. 213-246.

[8]Shur, M., Spalart, P.R., and Strelets, M.K., "Noise Prediction for Increasingly Complex Jets. Part II: Applications," *Inter J. Aeroacoustics*, Vol. 4, No. 3-4, 2005, pp. 247-266.

[9]Bogey, C. and Bailly, C., "A family of low dispersive and low dissipative explicit schemes for flow and noise computations," *J. Comp. Phys.*, Vol. 194, 2004, pp. 194-214.

[10]Bogey, C. and Bailly, C., "Effects of Inflow Conditions and Forcing on Subsonic Jet Flows and Noise," *AIAA J.*, Vol. 43, No. 5, 2005, pp. 1000-1007.

[11]Bogey, C. and Bailly, C., "Investigation of subsonic jet noise using LES: Mach and Reynolds number effects,"

AIAA Paper 2004-3023, Presented at the 10th AIAA/CEAS Aeroacoustics Conference, Manchester, U.K., 10-12 May, 2004.

[12]Bogey, C. and Bailly, C., "LES of a High Reynolds, High Subsonic Jet: Effects of the Inflow Conditions on Flow and Noise," AIAA Paper 2003-3170, Presented at the 9th AIAA/CEAS Aeroacoustics Conference and Exhibit, May 12-14, 2003, Hilton Head, South Carolina, 2003.

[13]Bogey, C. and Bailly, C., "LES of a High Reynolds, High Subsonic Jet: Effects of the Subgrid Modellings on Flow and Noise," AIAA Paper 2003-3557, Presented at the 16th AIAA Computational Fluid Dynamics Conference, June 23-26, 2003, Orlando, Florida, 2003.

[14]Ahuja, K.K., Lepicovsky, J., Tam, C.K.W., Morris, P.J., and Burrin, R.H., "Tone-Excited Jet: Theory and Experiments," Tech. Rep. NASA CR-3538, NASA, Nov. 1982.

[15]Bridges, J. and Wernet, M.P., "Measurements of the aeroacoustic sound source in hot jets," AIAA Paper 2003-3130, Presented at the 9th AIAA/CEAS Aeroacoustics Conference and Exhibit, Hilton Head Island, SC, May 12-14, 2003.

[16]Shur, M., Spalart, P.R., and Strelets, M.K., "Further steps in LES-based noise predicition for complex jets," AIAA Paper 2006-485, AIAA 44th Aerospace Sciences Meeting and Exhibit, 9-12 January, 2006, Reno, NV.

[17]Ladeinde, F., Cai, X., Alabi, K., and Safta, C. "The first high-order simulation of realistic aerospace systems" AIAA Paper 2006-1526, AIAA 44th Aerospace Sciences Meeting and Exhibit, 9-12 January, 2006, Reno, NV.

[18]Cai, X., Ladeinde, F. and Alabi, K., "Towards predicting supersonic, hot jet noise", AIAA 2007-0826.

[19]Suzuki, T. and Colnius, T. "Instability waves in a subsonic round jet detected using a near-field microphone array, " J. Fluid Mech. Vol. 565, pp. 192-226.

[20]Bogey, C. and Bailly, C., "Contributions of computational aeroacoustics to jet noise research and prediction." Int. J. Computational Fluid Dynamics, Vol. 18 (6), pp. 481-491, 2004.

[21]Bodony, D.J. and Lele, S., "On using large eddy simulation for the prediction of noise from cold and heated turbulent jets," Physics of Fluids 17, 2005.

[22]Bridges, J. and Wernet, M.P., "Measurements of the aero-acoustic sound source in hot jets," AIAA-2003-3130.

[23]Witze, P.O, "Centerline velocity decay of compressible free jets," AIAA J. 12, 417(1974).

[24]Reba, R, Narayanan, S., Colonius, T., and Suzuki, T. "Modeling jet noise from organized structures using near-field hydrodynamic pressure," 11th AIAA/CEAS Aeroacoustics Conference, Monterey, California, AIAA paper 2005-3093

[25]Panda J. et al., "Effect of heating on turbulent density fluctuations and noise generation from high-speed jets," NASA/TM-2004-213126